Available online at www.sciencedirect.com
ScienceDirect
Trans. Nonferrous Met. Soc. China 20(2010) 1439−1446
Transactions of Nonferrous Metals Society of China
www.tnmsc.cn

Influence of rapid quenching on hydrogen storage characteristics of nanocrystalline Mg_2Ni-type alloys

ZHANG Yang-huan (张羊换)[1, 2], ZHAO Dong-liang (赵栋梁)[1], LI Bao-wei (李保卫)[2], GUO Shi-hai (郭世海)[1], QI Yan (祁 焱)[1], WANG Xin-lin (王新林)[1]

1. Department of Functional Material Research, Central Iron and Steel Research Institute, Beijing 100081, China;
2. School of Materials, Inner Mongolia University of Science and Technology, Baotou 014010, China

Received 8 August 2009; accepted 10 May 2010

Abstract: Nanocrystalline Mg_2Ni-type alloys with nominal compositions of $Mg_{20}Ni_{10-x}Cu_x$ (x = 0, 1, 2, 3, 4, mass fraction, %) were synthesized by rapid quenching technique. The microstructures of the as-cast and quenched alloys were characterized by XRD, SEM and HRTEM. The electrochemical hydrogen storage performances were tested by an automatic galvanostatic system. The hydriding and dehydriding kinetics of the alloys were measured using an automatically controlled Sieverts apparatus. The results show that all the as-quenched alloys hold the typical nanocrystalline structure and the rapid quenching does not change the major phase Mg_2Ni. The rapid quenching significantly improves the electrochemical hydrogen storage capacity of the alloys, whereas it slightly impairs the cycling stability of the alloys. Additionally, the hydrogen absorption and desorption capacities of the alloys significantly increase with rising quenching rate.

Key words: Mg_2Ni-type alloy; rapid quenching; hydrogen storage characteristic

1 Introduction

Mg and Mg-based metallic hydrides are considered as the most promising materials for hydrogen storage because of their high hydrogen capacity and low price[1−2]. Unfortunately, some shortcomings of these kinds of metal hydrides, such as slow sorption−desorption kinetics, high dissociation temperature and poor electrochemical cycling properties, limit their practical application. Therefore, finding ways of improving the hydration kinetics of Mg-based alloys has been one of the main challenges faced by researchers in this area. Various attempts, involving mechanical alloying (MA)[3], GPa hydrogen pressure method[4], melt spinning[5], gravity casting[6], polyol reduction[7], hydriding combustion synthesis[8], surface modification[9], alloying with other elements[10], adding catalysts[11] etc, have been undertaken to improve the activation and hydriding properties.

ZALUSKA et al[12] reported that a milled mixture of Mg_2NiH_4 and MgH_2 shows the excellent absorption−desorption kinetics at 220–240 °C and a maximum hydrogen content of more than 5%. HANADA et al[13] obtained a hydrogen storage capacity of 6.5% after doping MgH_2 with nanosized-Ni in a temperature range of 150–250 °C. RECHAM et al[14] found that the hydrogen absorption property of ball-milled MgH_2 can be enhanced by adding NbF_5, and MgH_2+5%NbF_5(mass fraction, the same below if not mentioned) composite desorbs 3 % of H_2 at 150 °C. CUI et al[15] confirmed that amorphous and/or nanocrystalline Mg-Ni-based alloys can electrochemically absorb and also desorb large amounts of hydrogen at room temperature. KOHNO et al[16] obtained a large discharge capacity of 750 mA·h/g at a current density of 20 mA/g for modified Mg_2Ni alloys.

However, the milled Mg and Mg-based alloys show very poor hydrogen absorbing and desorbing stability due to the fact that the metastable structures formed by ball milling tend to vanish during multiple hydrogen absorbing and desorbing cycles[17]. Alternatively, rapid quenching technique can overcome the above mentioned shortcoming and effectively avoide the significant

Foundation items: Project(2007AA03Z227) supported by High-tech Research and Development Program of China; Projects(50871050, 50701011) supported by the National Natural Science Foundation of China; Project(200711020703) supported by the Natural Science Foundation of Inner Mongolia, China; Project (NJzy08071) supported by High Education Science Research Project of Inner Mongolia, China
Corresponding author: ZHANG Yang-huan; Tel: +86-10-62187570; E-mail: zyh59@yahoo.com.cn
DOI: 10.1016/S1003-6326(09)60318-6

degradation of hydrogen absorbing and desorbing cycling properties of Mg and Mg-based alloys[18]. SPASSOV et al[19] prepared $Mg_2(Ni,Y)$ hydrogen storage alloy with exact composition $Mg_{63}Ni_{30}Y_7$ by rapid solidification, and its maximum hydrogen absorption capacity reached about 3.0 %. HUANG et al[20] found that amorphous and nanocrystalline Mg-based alloy $(Mg_{60}Ni_{25})_{90}Nd_{10}$ prepared by rapid quenching obtained the highest discharge capacity of 580 mA·h/g and the maximum hydrogen capacity of 4.2 %.

The aim of this work is to produce the nanocrystalline Mg-Ni-based ternary alloys by rapid quenching and to examine the influence of rapid quenching on hydrogen storage characteristics of nanocrystalline $Mg_{20}Ni_{10-x}Cu_x$ (x= 0, 1, 2, 3, 4) alloys.

2 Experimental

The nominal compositions of the experimental alloys were $Mg_{20}Ni_{10-x}Cu_x$(x=0, 1, 2, 3, 4, mass fraction, %). For convenience, the alloys were denoted with Cu content as Cu_0, Cu_1, Cu_2, Cu_3 and Cu_4, respectively. The alloy ingots were prepared using a vacuum induction furnace in a helium atmosphere at a pressure of 0.04 MPa. Part of the as-cast alloys were re-melted and spun by melt-spinning with a rotating copper roller. The spinning rate was approximately expressed by the linear velocity of the copper roller because it is too difficult to measure a real spinning rate, i.e. cooling rate of the sample during spinning. The spinning rates used in the experiment were 15, 20, 25 and 30 m/s, respectively.

The morphologies of the as-cast alloys were examined with scanning electronic microscope (SEM) (Philips QUANTA 400). The phase structures of the as-cast and spun alloys were determined with XRD diffractometer (D/max/2400). The diffraction, with the experimental parameters of 160 mA, 40 kV and 10 (°)/min respectively, was performed with Cu K_α radiation filtered by graphite. The thin film samples of the as-spun alloys were prepared by ion etching for observing the morphology with high resolution transmission electronic microscope (HRTEM) (JEM-2100F, operated at 200 kV), and for determining the crystalline state of the samples with electron diffraction (ED).

The alloy ribbons were pulverized and then mixed with carbonyl nickel powder in a mass ratio of 1:4. The mixture was cold pressed into round electrode pellets of 10 mm in diameter and total mass of about 1 g with a pressure of 35 MPa. A tri-electrode open cell, consisting of a metal hydride electrode, a sintered $NiOOH/Ni(OH)_2$ counter electrode and a Hg/HgO reference electrode, was used for testing the electrochemical characteristics of the experimental alloy electrodes. A 6 mol/L KOH solution was used as the electrolyte. The voltage between the negative electrode and the reference electrode was defined as the discharge voltage. In every cycle, the alloy electrode was first charged at a current density of 20 mA/g; after resting for 15 min, it was discharged at the same current density to −0.500 V cut-off voltage. The environment temperature of the measurement was kept at 30°C .

The hydrogen absorption and desorption kinetics of the alloys were measured by an automatically controlled Sieverts apparatus. The hydrogen absorption was conducted at 1.5 MPa and the hydrogen desorption in a vacuum (1×10^{-4} MPa) at 200 °C.

3 Results and discussion

3.1 Microstructure characteristics

The SEM images of the as-cast alloy are shown in Fig.1, displaying a typical dendritic structure. The substitution of Cu for Ni does not change the morphology of the alloys but it causes a significant refinement of the grains. The result obtained by energy dispersive spectrometry (EDS) indicates that the major phase of the as-cast alloys is Mg_2Ni phase (denoted as A). Some small massive matters in the alloys containing Cu can clearly be seen in Fig.1, which is determined by EDS to be Mg_2Cu phase (denoted as B).

The XRD patterns of the as-cast and quenched Cu_2 and Cu_4 alloys are presented in Fig.2, showing that all the as-cast and quenched alloys display a single phase structure. This seems to be contrary with the result of SEM observation shown in Fig.1. It is most probably associated with the fact that Mg_2Ni and Mg_2Cu hold completely identical structure and nearly same lattice constants. On the other hand, the amount of the Mg_2Cu phase is very little so that the XRD observation cannot detect the presence of the Mg_2Cu phase. The lattice parameters are listed in Table 1. The cell volume and the full width at half maximum (FWHM) values of the main diffraction peaks of the as-cast and quenched Cu_2 and Cu_4 alloys were calculated by software of Jade 6.0. It can be derived from Table 1 that the rapid quenching makes the FWHM values of the main diffraction peaks of the alloys significantly increase and the lattice parameters and cell volume of the alloys cleverly enlarge, which is undoubtly attributed to the refinement of the average grain size and stored stress in the grains produced by rapid quenching. The crystallite size, D_{hkl} (Å) of the as-quenched alloy was calculated from the FWHM values of the broad diffraction peak (203) in Fig.2(b), using Scherrer's equation. The grain sizes of the as-quenched alloys are in a range of 2−6 nm, which are consistent with the results reported by FRIEDLMEIER et al [21].

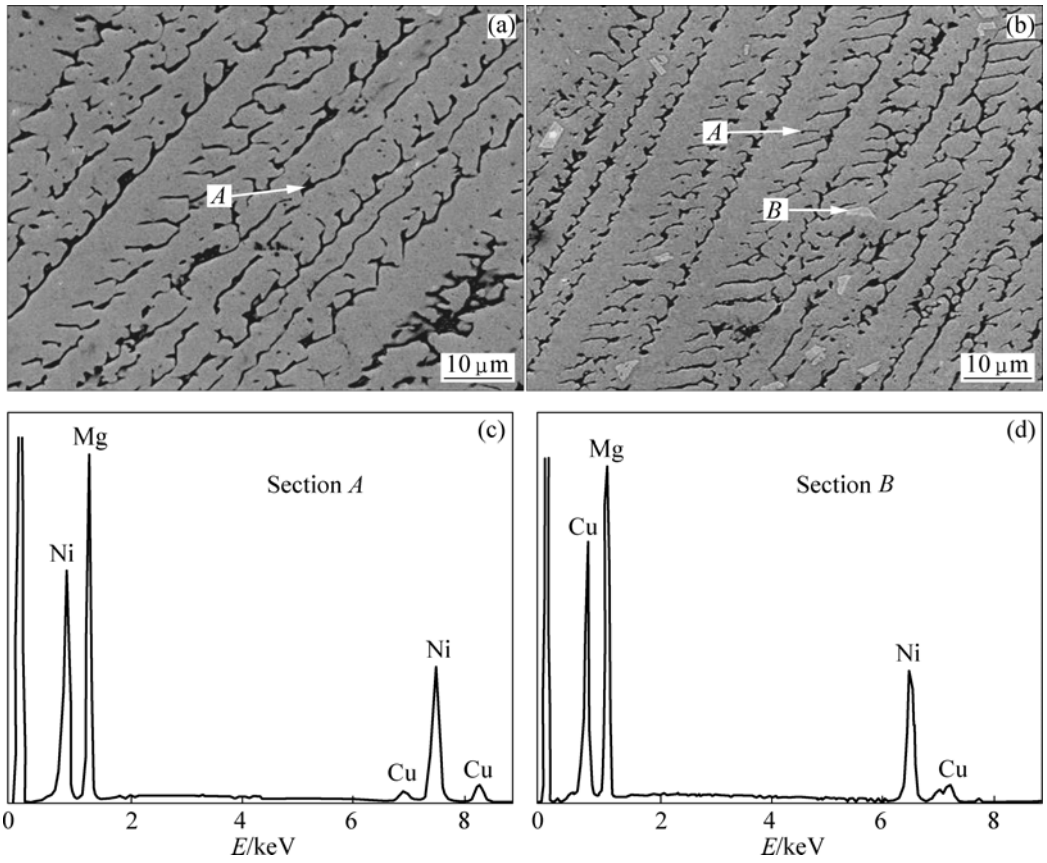

Fig.1 SEM images of as-cast Cu_0 alloy (a) and Cu_3 alloy (b), and typical EDS spectra of sections *A* (c) and *B* (d)

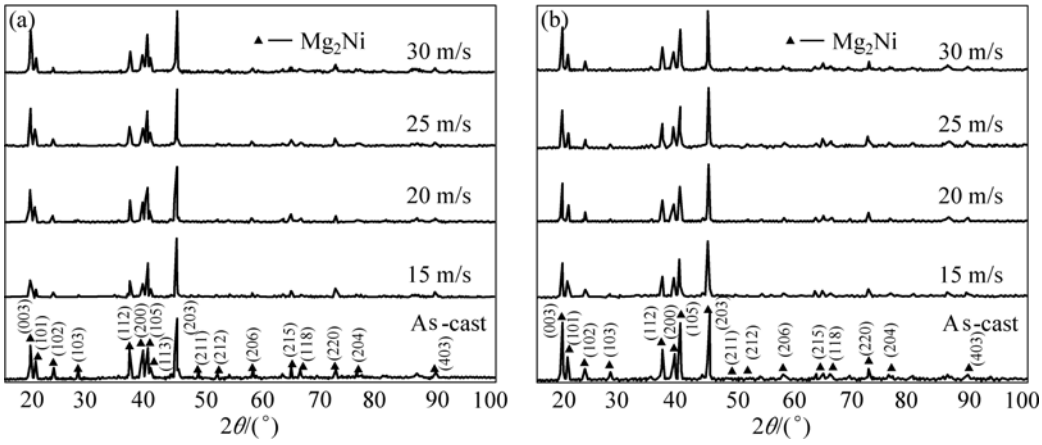

Fig.2 XRD patterns of as-cast and as-spun alloys: (a) Cu_2 alloy; (b) Cu_4 alloy

Table 1 Lattice parameters, cell volume and FWHM values of major diffraction peaks of alloys

Quenching rate/ ($m \cdot s^{-1}$)	FWHM values				Lattice parameters and cell volume					
	2θ=20.02°		2θ=45.14°		*a* /nm		*c* /nm		*V* /nm^3	
	Cu_2	Cu_4	Cu_2	Cu_4	Cu_2	Cu_4	Cu_2	Cu_4	Cu_2	Cu_4
0	0.148	0.165	0.183	0.204	0.5214	0.521 7	1.328 3	1.330 2	0.312 7	0.313 5
15	0.181	0.232	0.207	0.241	0.5216	0.522 0	1.329 3	1.331 1	0.313 2	0.314 1
20	0.232	0.286	0.223	0.252	0.5216	0.522 0	1.330 7	1.331 7	0.313 5	0.314 3
25	0.258	0.292	0.242	0.273	0.5217	0.522 1	1.331 1	1.332 3	0.313 8	0.314 5
30	0.274	0.305	0.259	0.285	0.5219	0.522 2	1.331 6	1.333 1	0.314 1	0.314 8

Fig.3 shows the HRTEM micrographs and electron diffraction patterns of the as-quenched Cu_2 and Cu_4 alloys, which displays a nanocrystalline microstructure, with an average crystal size of about 2–5 nm. From HRTEM observations, it can be found that the as-quenched alloys are strongly disordered and nanostructured, but no amorphous phase is detected in the alloys. This result agrees very well with the XRD observation shown in Fig.2. The crystal defects in the as-quenched alloy, dislocations (denoted as *A*), twin-grain boundaries (denoted as *B*), sub-grain boundaries (denoted as *C*) and stacking faults (denoted as *D*) formed by rapid quenching can clearly be seen in Fig.4.

3.2 Electrochemical hydrogen storage characteristics

3.2.1 Charging and discharging cycling stability

The cycling stability of the electrode alloy is a decisive factor of the life of the Ni-MH battery. The capacity retaining rate (S_n), which was introduced to accurately evaluate the cycling stability of the alloy, is defined as $S_n=(C_n/C_{max})\times100\%$, where C_{max} is the maximum discharge capacity and C_n is the discharge capacity of the nth charge−discharge cycle. The evolution of the capacity retaining rate (S_{20}) of the alloys with quenching rate is illustrated in Fig.5. It can be seen from Fig.5 that the capacity retaining rate (S_{20}) of the alloys clearly declines with rising quenching rate. When quenching rate increases from 0 (As-cast was defined as quenching rate of 0 m/s) to 30 m/s, the capacity retaining rate after 20 cycles falls from 58.6% to 42.3% for the Cu_2 alloy, and from 74.4% to 51.1% for the Cu_4 alloy. It can also be seen in Fig.5 that, for a fixed quenching rate, the capacity retaining rate of the alloys mounts up with rising Cu content, reflecting that the substitution of Cu for Ni enhances the cycling stability of the alloys. In order to clearly see the process of the capacity degradation of the alloy electrode, the evolution of the capacity retaining rate of the as-cast and as-quenched Cu_2 and Cu_4 alloys with the cycle number is shown in Fig.6. A rough tendency can be seen in Fig.6 that the rapid quenching causes an increase of the decay rates of the discharge capacities of the alloys, suggesting that the rapid quenching impairs the cycling stability of the alloys. It is well known that the essential reason for the capacity degradation of the Mg-based alloy electrodes is the severe corrosion of Mg in the alkaline KOH solution. Especially, during the discharging process, the alloys are

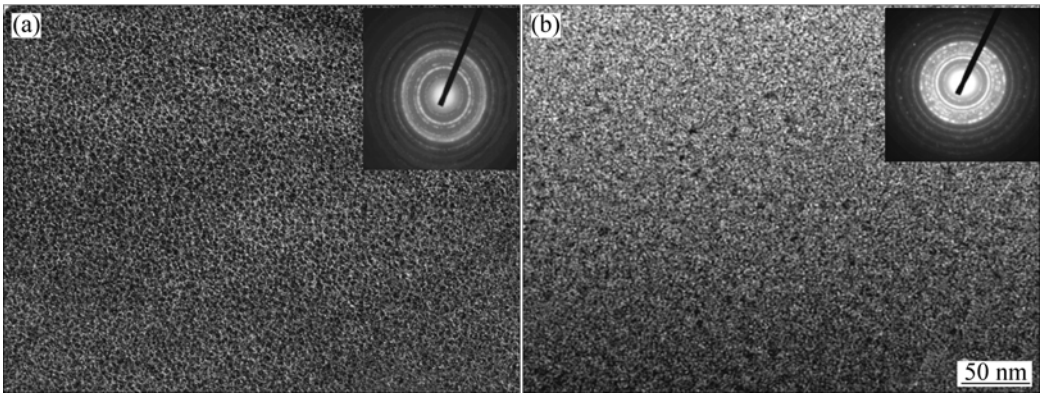

Fig.3 HRTEM micrographs and ED of as-spun alloys (30 m/s): (a) Cu_2 alloy; (b) Cu_4 alloy

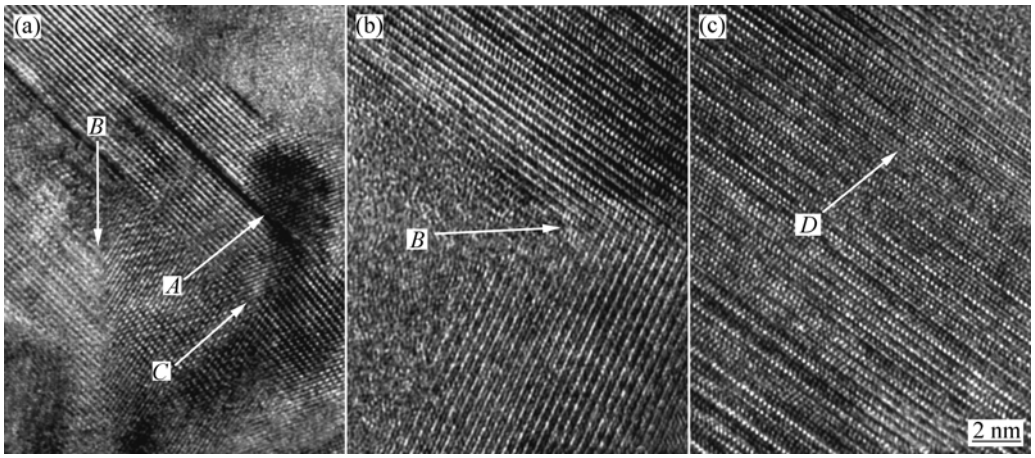

Fig.4 Crystal defects in as-spun (30 m/s) Cu_4 alloy taken by HRTEM: (a) Dislocations, sub-grain boundary and twin-grain boundary; (b) Twin-grain boundary; (c) Stacking faults

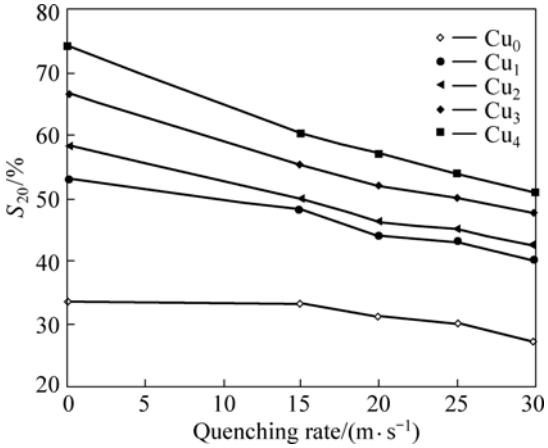

Fig.5 Evolution of capacity retaining rate (S_{20}) of alloys with quenching rates

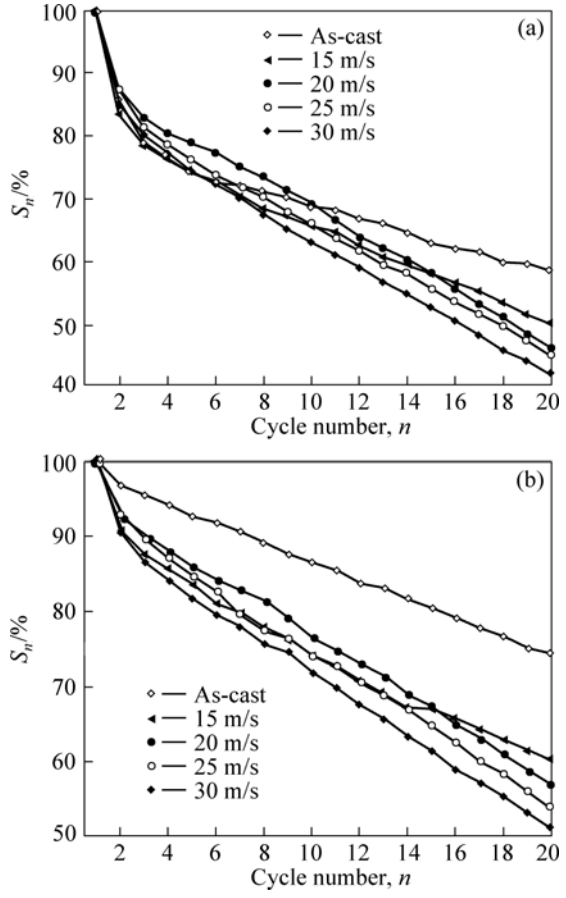

Fig.6 Evolution of capacity retaining rate of as-cast and as-quenched Cu_2 alloy (a) and Cu_4 alloy (b) with cycle number

anodically polarized so that corrosion would be faster[2]. On the other hand, the metastable structures formed by melt spinning or ball milling tend to vanish during multiple charging−discharging cycles, which is an important factor for the capacity decay of the alloys. Two reasons are responsible for the enhanced cycle stability of the Mg_2Ni-type alloy by Cu substitution. Firstly, the improved performance in the cycling life of substituted alloy electrodes is presumably attributed to the preferential oxidation of Cu on the alloy surface and the prevention of the formation of the $Mg(OH)_2$ passive layer[2]. Secondly, the addition of third alloying element significantly stabilizes the nanostructure of Mg-Ni-based alloy[19], reflecting an increase of the cycling stability of the alloy. The nanostructure of the alloys formed by rapid quenching is detrimental for corrosion in the electrolyte during cycling due to the fact that intercrystalline corrosion is inevitable. Therefore, it is comprehensible why rapid quenching leads to a decline of the cycling stability of the Mg-Ni-Cu system alloy.

3.2.2 Activation capability and discharge capacity

Electrochemical galvanostatic charge−discharge is a more effective and less time-consuming method for determining the absorbing hydrogen capacity than a gaseous technique. The influence of rapid quenching on the activation capability of the alloys is shown in Fig.7, as the charging−discharging current density is 20 mA/g. It can be seen that all the alloys have excellent activation capabilities and attain their maximum discharge capacities at first charging−discharging cycle. The rapid quenching does not affect the activation performances of the alloys. The evolution of the maximum discharge capacities of the alloys with the quenching rate is shown

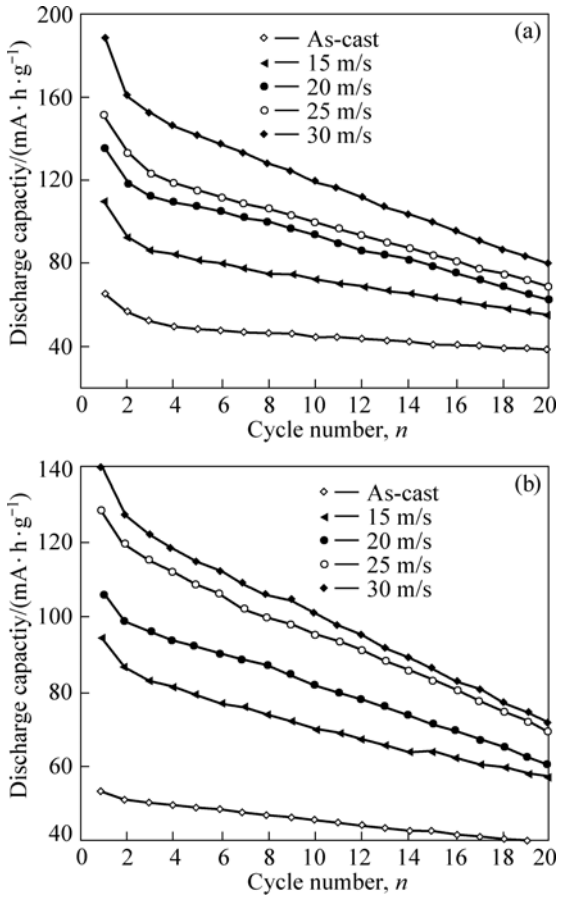

Fig.7 Evolution of discharge capacity of alloys with cycle number: (a) Cu_2 alloy; (b) Cu_4 alloy

in Fig.8. It can be derived in Fig.8 that the discharge capacity of the alloys increases with rising quenching rate. When the quenching rate increases from 0 to 30 m/s, the discharge capacity enhances from 65.9 to 189.3 mA·h/g for the Cu_2 alloy, and from 53.3 to 140.4 mA·h/g for Cu_4 alloy. A similar result was reported by SIMIČIĆ et al[2].

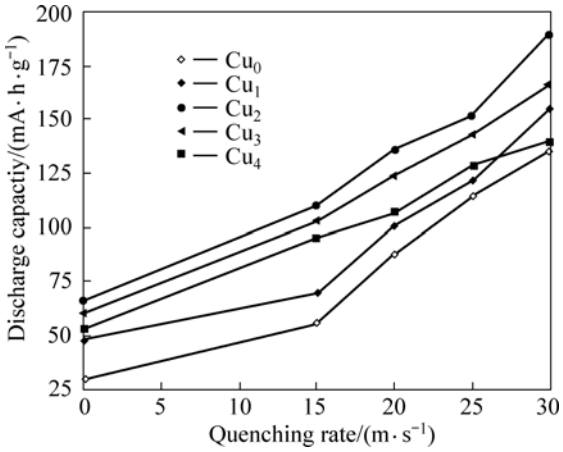

Fig.8 Evolution of discharge capacity of alloys with quenching rate

It must be mentioned that the discharge capacity of the alloys containing Cu is higher than that of Cu-free alloy, suggesting that the substitution of Cu for Ni enhances the discharge capacity of the Mg_2Ni-type alloy. Two reasons are mainly responsible for this result. Firstly, the partial substitution of Cu for Ni in Mg_2Ni compound may help to destabilize the hydride and activate the Mg_2Ni phase to absorb/desorb reversibly hydrogen in the alkaline electrolyte[2]. On the other hand, the secondary phase Mg_2Cu probably acts as an efficient catalyst for dissociating H_2 molecules and transferring the H atoms to the surrounding Mg_2Ni matrix[17]. The observed essential differences in the discharge capacity of the alloys caused by rapid quenching most probably are associated with the differences in their microstructures. The crystalline material, when being rapidly quenched, becomes at least partially disordered and its structure changes to nanocrystalline. Consequently, high densities of crystal defects such as dislocations, stacking faults and grain boundaries are introduced. The densities of the crystal defects mainly depend on the spinning rate. The higher the spinning rate is, the larger the densities of the crystal defects are. The large number of interfaces and grain boundaries available in the nanocrystalline materials provide easy pathway for hydrogen diffusion and accelerate the hydrogen absorbing/desorbing process. Additionally, as a result of the defects introducing distortion of crystal lattice, the stored sufficient energy as chemical disorder and the introduced defects (including stacking faults as well as grain boundaries) will produce internal strain. It was concluded by NIU and NORTHWOOD[22] that the exchange current density and H-diffusion coefficient are directly proportional to the internal strain. Therefore, it is understandable that the introduction of defects, disordering and internal strain leads to an increasing hydriding/dehydriding rates and capacity.

3.3 Hydriding and dehydriding kinetics

Fig.9 shows the hydrogen absorption capacity and kinetics of the as-cast and as-quenched Cu_2 and Cu_4 alloys. It can be seen that all hydriding kinetic curves of the as-quenched alloys show an initial fast hydrogen absorption stage after which the hydrogen content is saturated at longer hydrogenation time, indicating that the rapid quenching significantly improves the hydrogen absorption property of the alloys. The hydrogen absorption capacities of the alloys increase with rising spinning rate. When the quenching rate grows from 0 to 30 m/s, the hydrogen absorption capacity of the Cu_2 alloy in 10 min rises from 2.33% to 3.24%, and from 1.54% to 2.72% for the Cu_4 alloy. The enhanced hydrogenation property by rapid quenching is undoubtedly associated with the refinement of the grains produced by rapid quenching[23]. By refining the microstructure, a lot of new crystallites and grain

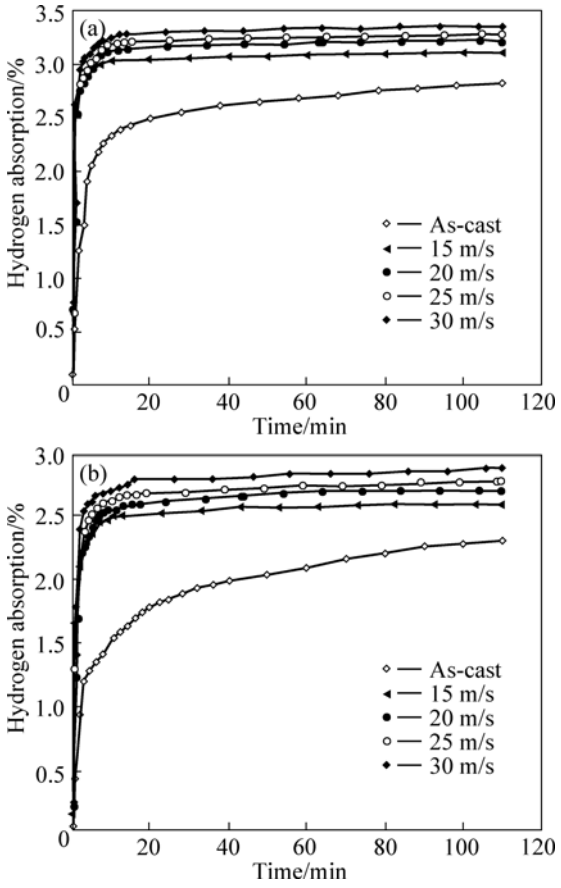

Fig.9 Hydrogen absorption kinetic curves of as-cast and as-quenched alloys: (a) Cu_2 alloy; (b) Cu_4 alloy

boundaries are created, which can act as fast diffusion paths for hydrogen absorption. ORIMO and FUJII[24] reported that the maximum hydrogen concentrations existed in three nanometer-scale regions, i.e. grain region and grain boundary region as well as amorphous region, and the corresponding values were 0.3% H, 4.0% H and 2.2% H, respectively. This reveals that the hydrides mainly exist in grain-boundary region and the amorphous phase region. The improved hydrogenation characteristics can be explained with the enhanced hydrogen diffusivity in the nanocrystalline microstructure as the nanocrystalline leads to an easier access of hydrogen to the nanograins, avoiding the long-range diffusion of hydrogen through an already formed hydride, which is often the slowest stage of absorption. It is known that the nanocrystalline microstructures can accommodate higher amounts of hydrogen than polycrystalline ones. The large number of interfaces and grain boundaries available in the nanocrystalline materials provide easy pathway for hydrogen diffusion and promote the absorption of hydrogen.

Fig.10 shows the hydrogen desorption capacity and kinetics of the as-cast and as-quenched Cu_2 and Cu_4 alloys, indicating that the dehydriding capability of the alloys obviously increases with rising quenching rate.

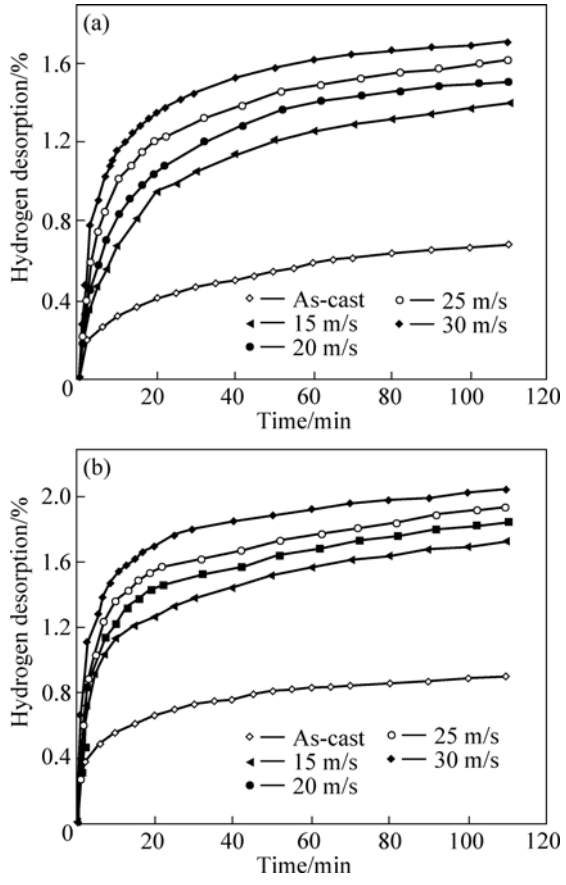

Fig.10 Hydrogen desorption kinetic curves of as-cast and as-quenched alloys: (a) Cu_2 alloy; (b) Cu_4 alloy

When the quenching rate grows from 0 to 30 m/s, the hydrogen desorption capacity of the Cu_2 alloy in 20 min increases from 0.42% to 1.35%, and from 0.65% to 1.68% for Cu_4 alloy, respectively. The nanocrystalline Mg_2Ni-based alloys produced by rapid quenching exhibit higher H-absorption capacity and faster kinetics of hydriding/dehydriding than crystalline Mg_2Ni. A similar result was reported by SPASSOV and KÖSTER[19]. The specific capacity and hydriding/dehydriding kinetics of hydride materials depend on their chemical composition and crystalline structure[25]. The observed essential differences in the hydriding/dehydriding kinetics of the as-quenched nanocrystalline Mg_2Ni-type alloys studied are most probably associated with the composition of the alloys as well as with the differences in their microstructure due to the different quenching rates. It was reported that the high surface to volume ratios, i.e. high specific surface area, and the presence of large number of grain boundaries in nanocrystalline alloys enhance the kinetics of hydrogen absorption/ desorption[19]. ZALUSKI et al[26] and ORIMO et al[27] confirmed that the hydriding/dehydriding characteristics at low temperatures (lower than 200 °C) of nanocrystalline Mg_2Ni alloys prepared by mechanical alloying can be improved by reducing the grain size (20–30 nm), due to hydrogen occupation in the disordered interface phase.

4 Conclusions

1) All the as-quenched $Mg_{20}Ni_{10-x}Cu_x$ (x=0, 1, 2, 3, 4) alloys hold nanocrystalline structures and are free of amorphous phase. The rapid quenching does not change the major phase of Mg_2Ni-type in the alloy, but it leads to an increment of the lattice parameters and cell volume as well as the FWHM values of the major diffraction peaks of the alloys.

2) Rapid quenching significantly improves the hydriding and dehydriding properties of the alloys. Hydriding and dehydriding capacities and rates of the alloy markedly rise with increasing spinning rate.

3) Additionally, rapid quenching considerably enhances the electrochemical discharge capacity of the alloys, whereas it slightly weakens the charging−discharging cycling stability of the alloys, for which the nanocrystalline structure formed by rapid quenching is basically responsible.

References

[1] SCHLAPBACH L, ZÜTYEL A. Hydrogen-storage materials for mobile applications [J]. Nature, 2001, 414: 353−358.

[2] SIMIČIĆ M V, ZDUJIĆ M, DIMITRIJEVIĆ R, NIKOLIĆ-BUJANOVIĆ Lj, POPOVIĆ N H. Hydrogen absorption and electrochemical properties of Mg_2Ni-type alloys synthesized by

mechanical alloying [J]. J Power Sources, 2006, 158(2): 730−734.

[3] EBRAHIMI-PURKANI A, KASHANI-BOZORG S F. Nanocrystalline Mg_2Ni-based powders produced by high-energy ball milling and subsequent annealing [J]. J Alloys Comp, 2008, 456: 211–215.

[4] KYOI D, SAKAI T, KITAMURA N, UEDA A, TANASE S. Synthesis of FCC Mg-Ta hydrides using GPa hydrogen pressure method and their hydrogen-desorption properties [J]. J Alloys Comp, 2008, 463: 306–310.

[5] PALADE P, SARTORI S, MADDALENA A, PRINCIPI G, RUSSO S L, LAZARESCU M, SCHINTEIE G, KUNCSER V, FILOTI G. Hydrogen storage in Mg-Ni-Fe compounds prepared by melt spinning and ball milling [J]. J Alloys Comp, 2006, 415: 170–176.

[6] SONG M Y, YIM C D, BAE J S , MUMMD D R, HONG S H. Preparation by gravity casting and hydrogen-storage properties of Mg-23.5 wt.%Ni-(5, 10 and 15 wt.%)La [J]. J Alloys Comp, 2008, 463: 143−147.

[7] HIMA KUMAR L, VISWANATHAN B, SRINIVASA MURTHY S. Hydrogen absorption by Mg_2Ni prepared by polyol reduction [J]. J Alloys Comp, 2008, 461: 72−76.

[8] LIU X F, ZHU Y F, LI L Q. Structure and hydrogenation properties of nanocrystalline Mg_2Ni prepared by hydriding combustion synthesis and mechanical milling [J]. J Alloys Comp, 2008, 455: 197−202.

[9] LIU F J, SUDA S. A method for improving the long-term storability of hydriding alloys by air water exposure [J]. J Alloys Comp, 1995, 231: 742−750.

[10] CZUJKO T, VARIN R A, CHIU C, WRONSKI Z. Investigation of the hydrogen desorption properties of Mg + 10 wt.% X (X =V, Y, Zr) submicrocrystalline composites [J]. J Alloys Comp, 2006, 414: 240−247.

[11] SAKINTUNA B, LAMARI-DARKKIM F, HIRSCHER M. Metal hydride materials for solid hydrogen storage: A review [J]. Int J Hydrogen Energy, 2007, 32: 1121−1140.

[12] ZALUSKA A, ZALUSKI L, STROEM-OLSEN J O. Synergy of hydrogen sorption in ball-milled hydrides of Mg and Mg_2Ni [J]. J Alloys Comp, 1999, 289: 197−206.

[13] HANADA N, ICHIKAWA T, FUJII H. Catalytic effect of nanoparticle 3d-transition metals on hydrogen storage properties in magnesium hydride MgH_2 prepared by mechanical milling [J]. J Phys Chem B, 2005, 109: 7188−7194.

[14] RECHAM N, BHAT V V, KANDAVEL M, AYMARD L, TARASCON J M, ROUGIER A. Reduction of hydrogen desorption temperature of ball-milled MgH_2 by NbF_5 addition [J]. J Alloys Comp, 2008, 464: 377−382.

[15] CNI N, LUAN B, ZHAO H J, LIU H K, DOU SX. Effects of yttrium additions on the electrode performance of magnesium-based hydrogen storage alloys [J]. J Alloys Comp, 1996, 233: 236−240.

[16] KOHNO T, KANDA M. Effect of partial substitution on hydrogen storage properties of Mg_2Ni alloy [J]. J Electrochem Soc, 1997, 144: 2384−2388.

[17] SONG M Y, KWON S N, BAE J S, HONG S H. Hydrogen-storage properties of Mg-23.5Ni-(0 and 5)Cu prepared by melt spinning and crystallization heat treatment [J]. Int J Hydrogen Energy, 2008, 33: 1711−1718.

[18] SAVYAK M, HIRNYJ S, BAUER H D, UHLEMANN M, ECKERT J, SCHULTZ L, GEBERT A. Electrochemical hydrogenation of $Mg_{65}Cu_{25}Y_{10}$ metallic glass [J]. J Alloys Comp, 2004, 364: 229−237.

[19] SPASSOV T, KÖSTER U. Thermal stability and hydriding properties of nanocrystalline melt-spun $Mg_{63}Ni_{30}Y_7$ alloy [J]. J Alloys Comp, 1998, 279: 279−286.

[20] HUANG L J, LIANG G Y, SUN Z B, WU D C. Electrode properties of melt-spun Mg-Ni-Nd amorphous alloys [J]. J Power Sources, 2006, 160(1): 684−687.

[21] FRIEDLMEIER G, ARAKAWA M, HIRAIA T, AKIBA E. Preparation and structural, thermal and hydriding characteristics of melt-spun Mg-Ni alloys [J]. J Alloys Comp, 1999, 292: 107−117.

[22] NIU H, NORTHWOOD D O. Enhanced electrochemical properties of ball-milled Mg_2Ni electrodes [J]. Int J Hydrogen Energy, 2002, 27: 69−77.

[23] TANAKA K, KANDA Y, FURUHASHI M, SAITO K, KURODA K, SAKA H. Improvement of hydrogen storage properties of melt-spun Mg-Ni-RE alloys by nanocrystallization [J]. J Alloy Comp, 1999, 295: 521−525.

[24] ORIMO S, FUJII H. Materials science of Mg-Ni-based new hydrides [J]. Appl Phys A, 2001, 72:167−186.

[25] MULAS G, SCHIFFINI L, COCCO G. Mechanochemical study of the hydriding properties of nanostructured Mg_2Ni-Ni composites [J]. J Mater Res, 2004, 19: 3279−3289.

[26] ZALUSKI L, ZALUSKA A, STRÖM-OLSEN J O. Nanocrystalline metal hydrides [J]. J Alloys Comp, 1997, 253/254: 70−79.

[27] ORIMO S, FUJII H, IKEDA K. Notable hydriding properties of a nanostructured composite material of the Mg_2Ni-H system synthesized by reactive mechanical grinding [J]. Acta Mater, 1997, 45: 331−341.

(Edited by LI Xiang-qun)